CD4$^+$ T Cells and CD40 Participate in Selection and Homeostasis of Peripheral B Cells

Marc A. Schwartz,* Nikita S. Kolhatkar,* Chris Thouvenel,[†,‡] Socheath Khim,[†,‡] and David J. Rawlings[*,†,‡]

Control of peripheral B cell development and homeostasis depends critically on coordinate signals received through the BAFFRs and BCRs. The extent to which other signals contribute to this process, however, remains undefined. We present data indicating that CD4$^+$ T cells directly influence naive B cell development via CD40 signaling. Loss of CD4$^+$ T cells or CD40–CD40L interaction leads to reduced B cell homeostatic proliferation and hindered B cell reconstitution posttransplantation. Furthermore, we demonstrate that in the absence of CD40 signals, these events are modulated by BCR self-reactivity. Strikingly, murine models lacking CD40 reveal a broadly altered BCR specificity and limited diversity by both single-cell cloning and high-throughput sequencing techniques. Collectively, our results imply that any setting of T cell lymphopenia or reduced CD40 function, including B cell recovery following transplantation, will impact the naive B cell repertoire. *The Journal of Immunology*, **2014, 193: 3492–3502.**

Formation of a functional, diverse AgR repertoire is the primary goal of lymphocyte development (1). Following successful BCR surface expression, immature B cells with sufficient affinity for self-Ag are censored for autoreactivity via receptor editing or clonal deletion. After bone marrow (BM) export, developing B cells progress through transitional stages in the spleen to enter mature subsets including marginal zone (MZ) B cells located within the splenic marginal sinus and follicular mature (FM) B cells that recirculate through B cell follicles in secondary lymphoid tissues (2, 3). Most developing B cells do not survive the competition for entry into mature subsets (1, 4, 5). Negative selection by clonal deletion continues in the periphery as transitional cells that receive a sufficient BCR stimulus undergo apoptosis (2, 3, 6, 7). In addition, accumulating evidence indicates transitional B cells are positively selected following BCR engagement with self-ligand (8–15). Importantly, the signals that facilitate BCR-mediated selection of transitional cells and the Ags responsible for shaping the endogenous B cell repertoire remain unclear.

In addition to the BCR, transitional B cell development is promoted by the cytokine BAFF, produced predominantly by myeloid cells (16) and signaling via the BAFFR and transmembrane activator and CAML interactor (TACI) (17). BAFFR engagement results in activation of the alternative NF-κB pathway leading to prosurvival signaling via Mcl1, Bcl-xL, and A1 (16, 18). BCR signals act in concert with BAFFR stimulation to promote peripheral B cell survival via complex cooperative effects that include BCR-generated classical NF-κB (18) and PI3K (19) activation; maintenance of p100 substrate levels, required for BAFFR-driven alternative NF-κB activation (20); modulation of BAFFR expression (21); and BCR complex scaffolding of BAFFR-mediated Syk activation (22).

Notably, previous work also has implicated T cells in modulating transitional B cell development. In vitro data demonstrate early transitional B cells undergo apoptosis following BCR engagement but proliferate with CD40 costimulation (6), and CD40L is expressed at low levels on naive splenic CD4 T cells providing a source for CD40L-mediated activation of transitional B cells (23). Mice with defects in both Bruton's tyrosine kinase (Btk, a key BCR signaling protein) and CD40 have a profound reduction in peripheral B cell numbers compared with mice with either defect alone (24, 25), implying CD40 promotes survival in the absence of sufficient BCR signals. Additional studies have demonstrated altered V_H gene usage in athymic mice (26), reduced transitional cell maturation in athymic rats (27), impaired B cell development in Btk mutant nude mice (28–30), inability to mediate chronic graft versus host disease when B cells develop in the absence of CD4 T cells (31), increased autoreactivity of mature B cells from CD40L-deficient patients (32), and impaired B cell maturation in humanized mice lacking T cells (33).

In this study, we further explore how CD4 T cells, through CD40 signaling, contribute to transitional B cell development, function, and repertoire in both lymphopenic and physiologic settings. We demonstrate that T cells and CD40 substantially promote B cell proliferation in response to lymphopenia. Furthermore, we show that CD40 provides a selective advantage during transitional and, most notably, MZ B cell development. In addition, we provide

*Department of Immunology, University of Washington School of Medicine, Seattle, WA 98195; [†]Department of Pediatrics, University of Washington School of Medicine, Seattle, WA 98195; and [‡]Center for Immunity and Immunotherapies, Seattle Children's Research Institute, Seattle, WA 98101

Received for publication March 31, 2014. Accepted for publication August 5, 2014.

This work was supported by the National Heart, Lung, and Blood Institute; the National Institute of Child Health and Human Development; and the National Institute of Allergy and Infectious Diseases of the National Institutes of Health under Awards R01HL075453 (to D.J.R.), R01AI084457 (to D.J.R.), and R01AI071163 (to D.J.R.). This work was also supported by the Benaroya Family Gift Fund and a Cancer Research Institute predoctoral training grant (to M.A.S. and N.S.K.).

The content is solely the responsibility of the authors and does not necessarily represent the official views of the National Institutes of Health.

Address correspondence and reprint requests to Dr. David J. Rawlings, Center for Immunity and Immunotherapies, Seattle Children's Research Institute, 1900 Ninth Avenue, Seattle, WA 98101. E-mail address: drawling@u.washington.edu

The online version of this article contains supplemental material.

Abbreviations used in this article: ANA, anti-nuclear Ab; BM, bone marrow; Btk, Bruton's tyrosine kinase; FM, follicular mature; GC, germinal center; HEL, hen egg lysozyme; HP, homeostatic proliferation; IFA, immunofluorescence assay; KO, knockout; KREC, κ recombination excision circle; MDA, malondialdehyde; MZ, marginal zone; PC, phosphorylcholine; SPADE, species prediction and diversity estimation; TACI, transmembrane activator and CAML interactor; Tg, transgenic; WT, wild-type.

a comprehensive analysis of the impact of CD40 signals on the mature B cell repertoire using transgenic (Tg) BCR models, single-cell BCR cloning, and high-throughput BCR sequencing. These data demonstrate perturbations in BCR specificity–based selection in the absence of CD40. Collectively, our findings indicate that T cells and CD40 expression significantly impact transitional B cell development and selection, suggesting that alterations in these events may modulate subsequent B cell responses to infection and/or autoimmunity.

Materials and Methods

Mice

Ly.5.1$^+$ and Ly5.2$^+$ C57BL/6, μMT, Rag knockout (KO), CD40$^{-/-}$, CD40L$^{-/-}$, MyD88$^{-/-}$, TRIF$^{-/-}$, *xid*, tec/Btk DKO, MD4-Tg, M167-Tg, and Vk8-Tg mice were bred and maintained in the specific pathogen-free animal facility of Seattle Children's Research Institute and handled according to Institutional Animal Care and Use Committee–approved protocols. M167 H chain Tg mice (M167H Tg mice, line U243-4) were provided by J. Kenny and A. Lustig (National Institute on Aging, Bethesda, MD) and established as a M167H Tg/Tg homozygous breeding colony in the animal facility of the Albert Einstein College of Medicine (New York, NY) by S. Porcelli.

Reagents and Abs

Anti-murine Abs used in this study include Ly5.1 (A20), Ly5.2 (RA3-6B2), AA4.1 and CD62L (MEL-14; eBioscience); CD24 (M1/69), CD21 (7G6), B220 (RA3-6B2), IgD (11-26C.2A), and CD4 (RM4-5) from BD Biosciences; BAFFR (204406) and TACI (R&D Systems); BP1 (FG35.4), CD25 (PC61), CD62L (MEC-14), CD11c (N418), Gr-1 (RB6-8C5), and CD23 (B3B4) from Caltag Laboratories; IgM (1B4B1), κ (187.1), Λ (JC5-1), goat anti mouse IgG-, IgG2b-, IgG2c-, IgG3-HRP conjugated, and SA-HRP conjugated from Southern Biotechnology Associates; CD19 (ID3), NK.1 (PK136), IgM^a (DS-1), and CD8a (53-6.7) from BioLegend; and Cy5 anti-rabbit polyclonal IgG from Jackson ImmunoResearch Laboratories; and Alexa Fluor 647 anti-M167 (28-6-20) Rat IgG2a from by S. Porcelli.

Flow cytometry and cell sorting

As previously described (12), single-cell suspensions from BM, peripheral blood, and spleen were incubated with fluorescently labeled Abs, and data were collected on a FACSCalibur or LSR II (BD Biosciences) and analyzed using FlowJo software (Tree Star). Cell sorting was done using an Aria II; sort purities were >90% in all studies. B cell subsets were gated as in Ref. 12 using B220, CD21, and CD24 and shown in Fig. 1D. CD1d and CD23 were used to further divide MZ (CD1d^{hi}CD23^{low}) and MZ precursors (CD1d^{int}CD23^{hi}).

Adoptive cell transfer

CD43-depleted B cells were incubated with 0.05 μM CFSE, and 10×10^6 cells were transferred by tail vein injection into recipient mice.

T cell depletion

Mice were treated with i.p. injection of 250 μg anti-CD4 (GK1.5) or isotype control (rat IgG2b) Ab (University of California San Francisco Ab Core). Recipient mice were initially treated with anti-CD4 or isotype control Ab at 1 d prior to transplant (2 mo of age) and then treated weekly for 8 wk as described previously (34). CD4 depletion was confirmed via FACS analysis (Supplemental Fig. 1B).

BM transplantation

BM was harvested from wild-type (WT), CD40$^{-/-}$, M167-Tg, or CD40$^{-/-}$ × M167-Tg mice. BM from CD40$^{-/-}$ and WT mice was mixed at either a 65:35 or 90:10 ratio, and 5×10^6 total BM cells in PBS were injected i.v. into lethally irradiated (1050 cGy) μMT recipients. Purity of transferred cells was confirmed by flow cytometry as demonstrated in Supplemental Fig. 1C. BM from M167-Tg and CD40$^{-/-}$ × M167-Tg were mixed at a 50:50 ratio.

Real-time PCR

RNA was isolated from sorted cells using the RNeasy Micro kit (Qiagen) and converted into cDNA by reverse transcription (Superscript II; Invitrogen). Real-time PCR was performed using iCycler real-time PCR detection system with IQ SYBR Green Supermix (Bio-Rad). Ratios were calculated using mouse β_2-microglobulin as a control. Primers used were as follows: β_2-MicroglobulinFP, 5′-CTTCAGTCGTCAGCATGGCTGG-3′, and RP, 5′-GCAGTTCAGTATGTTCGGCTTCCC-3′; BAFFR FP, 5′-CTGAGGCTGCAGAGCTGTC-3′, and RP, 5′-GGTGAGAAACTGCGTGTCCT-3′; TACI FP, 5′-ACCCCCAGTGTGCAGTAGAG-3′, and RP, 5′-GGAGGTGGAAGTCAGGTCAG-3′; A1 FP, 5′-CCTGGCTGAGCACTACCTTCA-3′, and RP, 5′-CTGCATGCTTGGCTTGGA-3′; and Bcl-XL FP, 5′-CTGGGACACTTTTGTGGATCTCT-3′, and RP, 5′-GAAGCGCTCCTGGCCTTT-3′. To determine the replication history of B cells, genomic DNA was isolated from sorted populations and the ratio between the κ-deleting rearrangement (IRS1 to RS) and excision circles (κ recombination excision circle [KREC]) was determined by TaqMan-based (Applied Biosystems) real-time PCR (35).

In vitro cell activation studies

In vitro activation studies were performed as described previously (12, 36). Stimulating treatments included agonistic anti-CD40 Ab (10 μM) and anti-IgM (10 μM).

Single-cell BCR cloning

cDNA was obtained using Thermo Maxima First-Strand cDNA Kit, supplemented with 0.5% Igepal CA-630 (v/v) (Sigma-Aldrich) to a final volume of 12 μl/well. *Igh*, *Igk*, or *Igl* gene transcripts were amplified independently from cDNA with nested PCR or seminested PCR (*Igl*) using DreamTaq (Thermo), 2.5 μl cDNA as template, and 400 nM primers as published for *Igh* (37) or *Igk* and *Igl* (38) to a final volume of 25 μl/well. First-round PCR was performed at 94°C for 5 min, followed by 15 cycles of 94°C for 30s, 47°C (*Igk*) or 51°C (*Igh*) or 53°C (*Igl*) for 30 s, 72°C for 55 s, followed by 30 cycles of 94°C for 30 s, 50°C (*Igk*) or 56°C (*Igh*) or 58°C (*Igl*) for 30 s, 72°C for 55 s, and a final incubation of 72°C for 8 min. Round 2 PCR and sequencing, gene analysis, and Ig gene-specific PCR was performed under settings described previously (38). PCR products were cloned into expression vectors with human *IGG1*, *IGK*, or *IGL* constant regions (21). HEK293T cells in 100-mm plates at 70–80% confluency were transiently transfected with 4 μg of each H and L chain plasmid and 32 μg polyethyleneimine in an 888 μl solution of 10 mM HEPES (Fisher) and 150 mM NaCl (pH 7.05) (EMD). Cells were cultured with serum-free medium, and supernatant was extracted for Ab purification. Abs were purified using 400 μl Pierce protein A–agarose beads (Thermo) in 5 ml polypropylene gravity columns (Thermo). Purified Abs were quantified four times and averaged using the Nanodrop2000 Spectrophotometer (Thermo).

ELISA and anti-nuclear Ab screen

Abs were tested for anti-nuclear Ab (ANA) reactivity (Bio-Rad), according to the manufacturer's protocol, at 100 μg/ml and serially diluted 1:2, 1:4, and 1:10. Reactivity with insulin, LPS, phosphorylcholine (PC)-12, and dsDNA (Sigma-Aldrich) at 100 μg/ml was tested by ELISA with Abs at 10 μg/ml and serially diluted 1:5, 1:25, and 1:125. For ELISAs, 96-well Immuno plates (Nunc) were precoated (1 mg/ml) overnight at 4°C with dsDNA, insulin, LPS, MDA-BSA, or MDA-LDL (20P-MD L-105; Academy Bio-Medical). After blocking with 0.5% BSA/PBS, recombinant human Abs were added, and plates were incubated with mouse anti-human IgG-HRP (Southern Biotechnology Associates) (1:2000 dilution). ANA screens were performed using BD EIA kit, according to the manufacturer's instructions. Serum BAFF levels were measured using BAFF/BlySS Quantikine ELISA kit (R&D Systems). Pooled Abs (60 Abs/subset at total concentrations of 100 ng/μl, 1 μg/μl, and 10 ug/μl) were sent to the University of Texas Southwestern Microarray Core Facility for analysis on autoantigen arrays.

HEp-2 immunofluorescence assay tests

BD immunofluorescence assay (IFA) slides were used, according to the manufacturer's instructions. Slides were incubated with Abs for 30 min. Next, slides were incubated with FITC-conjugated anti-human IgG for 30 min. Coverslips were then added with mounting media, and images were acquired using a Leica DM6000B microscope, Leica DFL300 FX camera, and Leica Application Suite Advanced Fluorescence software.

High-throughput BCR sequencing

Total RNA was obtained from purified B cells using RNeasy reagents (Qiagen). H chain cDNAs from each sample were synthesized using a 5′-RACE kit (Ambion), according to the manufacturer's protocol. For reverse transcriptase and PCR, Transcriptor High Fidelity (Roche) and Phusion Hot Start (New England Biolabs) was used, respectively. A triple-nested primer strategy was used to amplify H chain IgM and IgD genes.

Outer IgM and IgD C region–specific primers were used for the reverse-transcription reaction, middle C region IgM and IgD primers were used for the first round of PCR, and innermost constant–region IgM and IgD primers (adjacent to the J segment of the V region) were used for the second PCR round. 454 adapters were included in the primers during second-round PCR, and a bar-code strategy was used to run multiple samples simultaneously. Sequencing was done at Mycroarray on a GS Junior. Bar-coded sequence data were separated using Geneious software, and IMGT/HighVQuest was used for alignment to germline IgH VDJ regions. IgAT software was used to generate descriptive statistics and calculate CDR3 characteristics (39). Software provided by Ramit Mehr's laboratory was used for clonal analysis and combination of clones from various samples. Species prediction and diversity estimation (SPADE) software was used for calculation of diversity indices (40).

Statistical evaluation

The *p* values were calculated using the two-tailed Student *t* test, ANOVA, or Fisher's exact test, where appropriate.

Results

$CD4^+$ T cells contribute to B cell homeostatic proliferation through CD40

The role of T cells and CD40 was first assessed in lymphopenia-induced B cell homeostatic proliferation (HP) as transitional B cells are preferentially expanded in this setting (Fig. 1A) (12). Compared with B cells transferred alone into RAG KO mice, cotransfer of $CD4^+$ T cells increased B cell HP (Fig. 1D); an effect abrogated when T cells lacked CD40L. Interestingly, transfer of both B and $CD40L^{-/-}$ T cells results in a slight increase in B cell proliferation; this is likely because of additional signals provided by donor T cells also undergoing homeostatic proliferation. As T cells undergo HP in RAG KO mice, we evaluated B cell HP using μMT-recipient mice. In this system, depletion of $CD4^+$ T cells, transfer of CD40-deficient B cells, or transfer of C57/BL6 WT B cells into CD40L-deficient μMT recipients each resulted in a ~50% reduction in proliferation (Fig. 1B, 1C). In contrast, depletion of $CD8^+$ T cells, inhibition of IL-4 (Fig. 1C), and deficiency of MyD88 or TRIF (data not shown) had no effect on B cell HP. Following transfer to lymphopenic recipients, recovered B cells exhibit a $CD21^{hi}CD24^{hi}$ phenotype, similar to MZ cells in unmanipulated animals. Loss of $CD4^+$ T cells or the CD40 pathway resulted in a portion of recovered cells with lower CD21 and CD24 levels (Fig. 1E), which could reflect impaired proliferation of a subset of B cells or could simply be a consequence of decreased proliferation of all transferred cells. These data demonstrate a major role for $CD4^+$ T cells, through CD40 signaling, in replenishing B cell numbers during lymphopenia.

The contribution of Ag-mediated BCR signals to B cell HP was addressed using M167-Tg mice in which a fraction of B cells contain a self-reactive PC-specific BCR recognizable by an Id-specific Ab (41). Compared with Id^- cells, Id^+ B cells exhibited increased HP (Fig. 1F). Although HP levels were reduced in Id^- cells with CD4 depletion, HP of Id^+ cells was unaffected by the presence of $CD4^+$ T cells (Fig. 1F). Collectively, these data point to independent roles for CD40- and BCR-induced signals during B cell HP.

Given the effect of CD40 on B cell HP, we evaluated whether CD40 plays a role in nonlymphopenic B cell development. As expected from prior observations, no difference was observed when quantifying peripheral B cell subsets in CD40 KO versus WT mice (data not shown). Cumulative division of FM and MZ B cells, assessed using the KREC assay, revealed no difference among WT, CD40 KO, and CD40L KO mice (Fig. 1G). Surface marker expression was largely comparable in WT and CD40-deficient B cells, although the MZ-precursor subset had lower MHC class II (data not shown). On the basis of the observations in CD40L-deficient patients (32), we measured serum BAFF levels and observed increased levels in both CD40L- and CD40-deficient mice (Fig. 1H). Taken together, these data suggest that CD40 deficiency results in a compensatory increase in circulating BAFF levels to maintain peripheral B cell numbers.

CD40 promotes peripheral B cell homeostasis in mixed BM chimeras

To assess development of WT versus $CD40^{-/-}$ B cells within an identical microenvironment, we generated mixed BM chimeras from congenically marked WT and $CD40^{-/-}$ BM (Fig. 2A). Generation of chimeras wherein the early transitional stage was composed of equal quantities of WT and $CD40^{-/-}$ B cells was accomplished at a 65:35 $CD40^{-/-}$:WT BM ratio. Analysis at 3 mo posttransplant revealed a progressive selective advantage for CD40-expressing cells beginning at the late transitional stage and most evident within the MZ subset (Fig. 2B). Depletion of $CD4^+$ T cells eliminated enrichment of WT cells in transitional and MZ-precursor subsets but only partially reduced enrichment within the MZ subset. A more stringent 90:10 $CD40^{-/-}$:WT BM ratio was used to further test competitive selection of WT B cells. In this setting, enrichment for WT cells in transitional stages was not observed indicating unperturbed BM B cell development, but the competitive advantage of CD40 expression remained in the MZ subset and was again reduced by CD4-T cell depletion (Fig. 2C). These data demonstrate that CD40 signals promote transitional B cell development and MZ subset homeostasis.

To evaluate how CD40 signals might mediate selection, surface levels of BAFF family receptors were analyzed as upregulation of these receptors coincides with developmental progression of transitional cells (42). BAFFR and TACI levels were increased in WT transitional cells derived from mixed BM chimeras, and this difference was abolished by CD4 depletion (Fig. 2D). Consistent with these data, in vitro stimulation of B cells with CD40 increased surface levels of BAFFR and TACI (Fig. 2E, 2F). Survival-associated genes *A1* and *BclxL* were increased in WT versus CD40-deficient early transitional cells (Fig. 2G). Thus, CD40 signals received through interaction with $CD4^+$ T cells promote upregulation of BAFF family receptors in transitional B cells suggesting that CD40 mediates its selective effect, at least in part, via increased BAFF signaling.

Because previous data indicate a subset of transitional cells is cycling in naive mice (3, 12), we asked whether CD40 promotes this process. Using DAPI and PyroninY to identify cells in S and G2 phases, the fraction of cycling cells was significantly enriched for WT cells versus CD40 KO cells in mixed chimeras (Fig. 2H). In contrast, KREC values did not differ between WT and $CD40^{-/-}$ FM and MZ subsets (Fig. 2I).

These data demonstrate that transitional B cells can receive $CD4^+$ T cell help through CD40, and this signal promotes the B cell developmental program by increasing expression of BAFFRs and survival genes, leading to a competitive advantage in entering mature B cell subsets, most notably the MZ compartment.

CD40 regulates B cell development when BCR signaling is impaired

Coordinate loss of CD40 and the BCR signaling effector, Btk, manifests as severe deficiency in naive B cell development (24, 25). To determine whether the impact of CD40 in this setting requires CD4 T cells, we depleted CD4 T cells from mice expressing mutant, nonfunctional Btk (*xid*) or lacking both Btk and the related kinase, Tec. In each strain, T cell depletion induced a block in transitional B cell development leading to near complete absence of FM and MZ subsets (Fig. 3A–D), whereas T cell de-

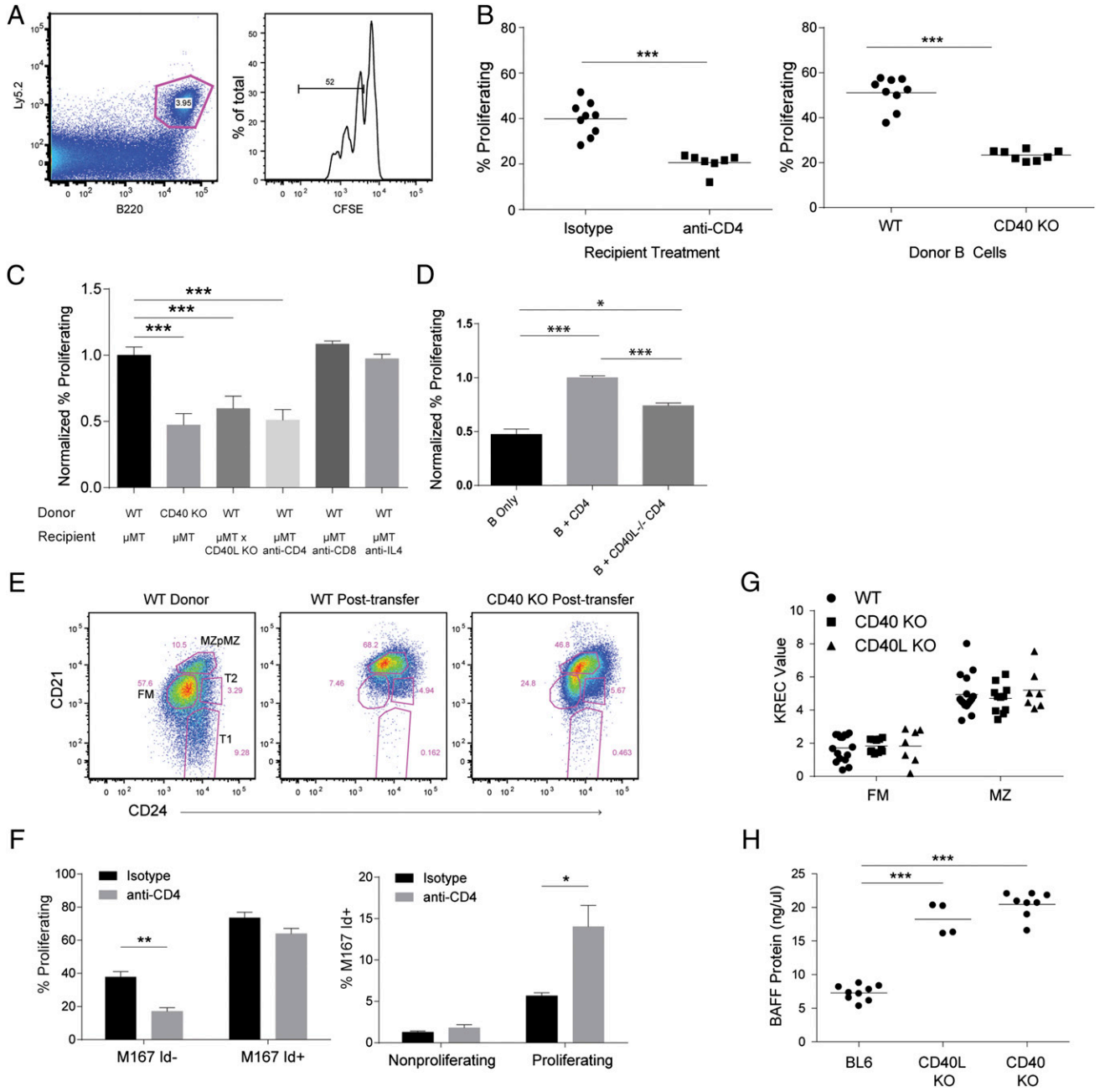

FIGURE 1. CD40 signaling promotes B cell HP. (A–E) B cell HP measured by transfer of splenic B cells into B cell–deficient μMT hosts. Ly5.2 congenically marked WT or CD40 KO B cells were transplanted in Ly5.1 μMT–recipient mice (**A**) Gating on congenically marked donor B cells (*left panel*) and proliferating cells by CFSE dilution (*right panel*). (**B**) B cell HP measured 5–7 d after transfer of WT B cells to μMT mice. *Left panel*, Mice receiving WT B cells were treated with either isotype control or CD4-depleting Ab. *Right panel*, Transfer of WT versus CD40 KO B cells to μMT recipients. (**C**) Summary of HP data from multiple experiments, data are normalized to either WT B cells or isotype control treated recipients for each individual experiment. (**D**) Transfer of B cells and/or CD40 sufficient or deficient $CD4^+$ T cells into Rag KO recipients. (**E**) Surface phenotype of WT donor B cells prior to transfer into μMT recipients for HP experiment (*left panel*) and after HP (*middle panel*); CD40 KO B cells after HP (*right panel*). (**F**) HP experiment using donor B cells from M167-Tg mice, showing proliferation of Id^- and Id^+ cells (*left panel*) and the frequency of Id^+ cells in nonproliferating or proliferating cells (*right panel*). (**G**) KREC assay on sorted FM and MZ cells from WT, CD40 KO, and CD40L KO mice. (**H**) Serum BAFF levels measured by ELISA in WT, CD40 KO, and CD40L KO mice. Error bars show SEM. Data representative of at least three experiments. $*p < 0.05$, $**p < 0.005$, $***p < 0.0005$.

pletion in WT mice had no effect (data not shown). As a separate model of reduced Ag-mediated BCR signaling, we generated CD40-deficient hen egg lysozyme (HEL)–specific MD4-Tg mice. This approach allowed us to determine whether CD40 affects development of a B cell population unable to recognize self-Ag. Although subset distribution did not change, absolute peripheral B cell numbers markedly decreased in CD40-deficient MD4 mice (Fig. 3E). Thus, in the absence of a sufficient signal through the BCR, transitional B cells are reliant on CD40–CD40L interactions to enter the mature B cell compartment.

Increased self-Ag–mediated positive selection of MZ B cells in the absence of CD40

Next, we tested whether CD40 deficiency alters positive selection of B cells expressing a self-reactive BCR. Using the M167-Tg model, we looked for selective enrichment of late-transitional,

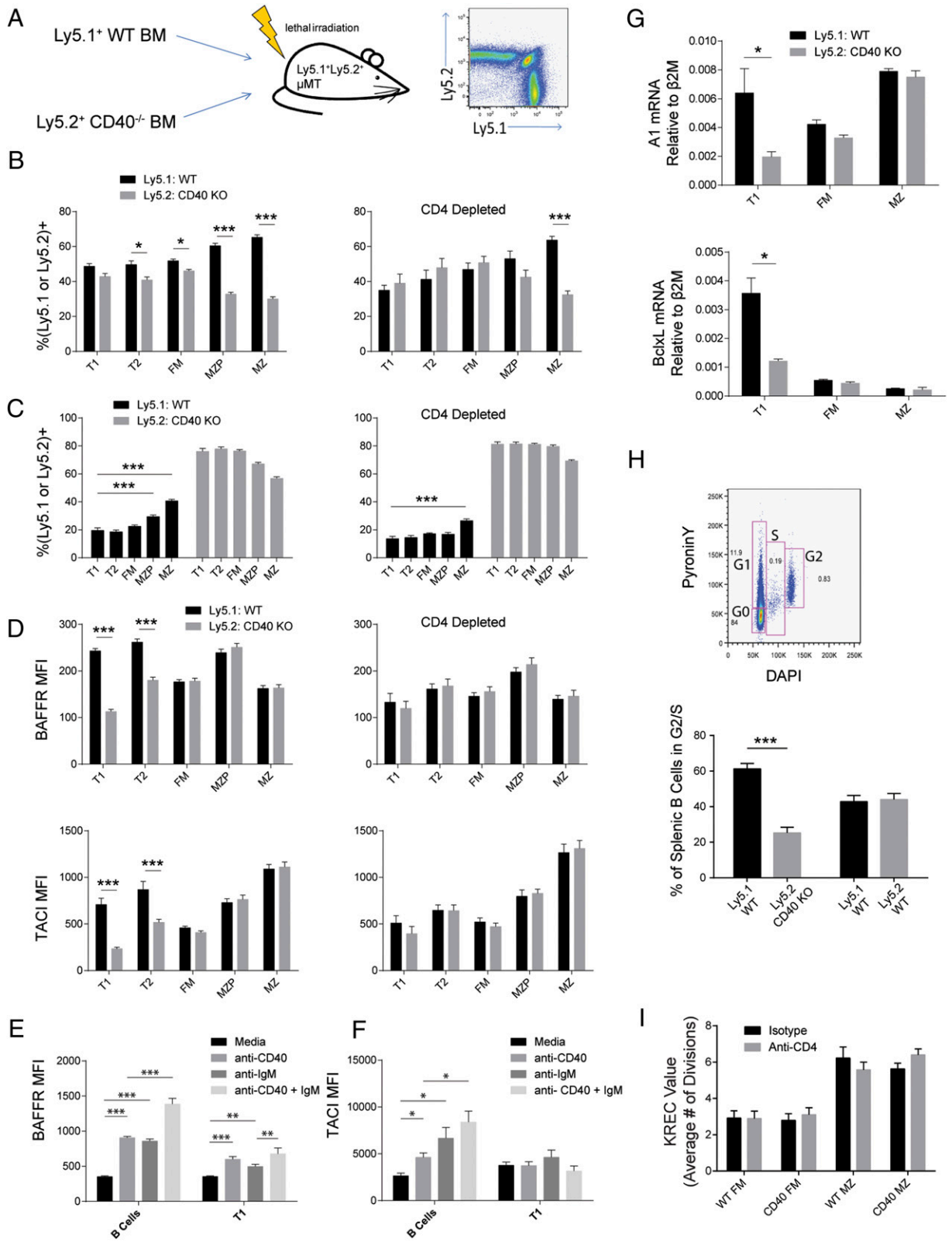

FIGURE 2. CD40 signaling promotes B cell development in mixed BM chimeras. (**A**) WT/CD40 KO–mixed BM chimeras created by transfer of congenically marked BM to µMT recipients. (**B**) The percentage of ly5.1$^+$ (WT) and ly5.2$^+$ (CD40 KO) cells in each B cell subset at 3 mo posttransplant using a 65:35 (CD40 KO:WT) ratio of donor BM, either untreated (*left panel*) or depleted of CD4 T cells (*right panel*); $n = 23$ mice. (**C**) Analysis of BM chimeras created with a 90:10 (CD40 KO:WT) ratio of donor BM, untreated (*left panel*), or depleted of CD4 T cells (*right panel*); $n = 26$ mice. (**D**) Mean BAFFR and TACI surface expression in BM chimeras created using both ly5.1$^+$ (WT) and ly5.2$^+$ (CD40 KO) WT donors, either untreated (*left panels*) or depleted of CD4 T cells (*right panels*); $n = 26$ mice. Surface expression of BAFFR (**E**) and TACI (**F**) after in vitro stimulation of B cells with agonistic anti-CD40 and anti-IgM Abs. (**G**) Quantitative PCR of subsets sorted from mixed BM chimeras; mRNA levels of A1 (*top panel*) and BclxL (*bottom panel*) relative to β_2-microglobulin. (**H**) Cell cycle analysis by DAPI and PyroninY staining; percentage of cells in a combined S and G2 gate in WT/CD40 KO chimeras and control chimeras created using WT ly5.1$^+$ and WT ly5.2$^+$ BM. (**I**) KRECs assay on FM and MZ cell subsets sorted (*Figure legend continues*)

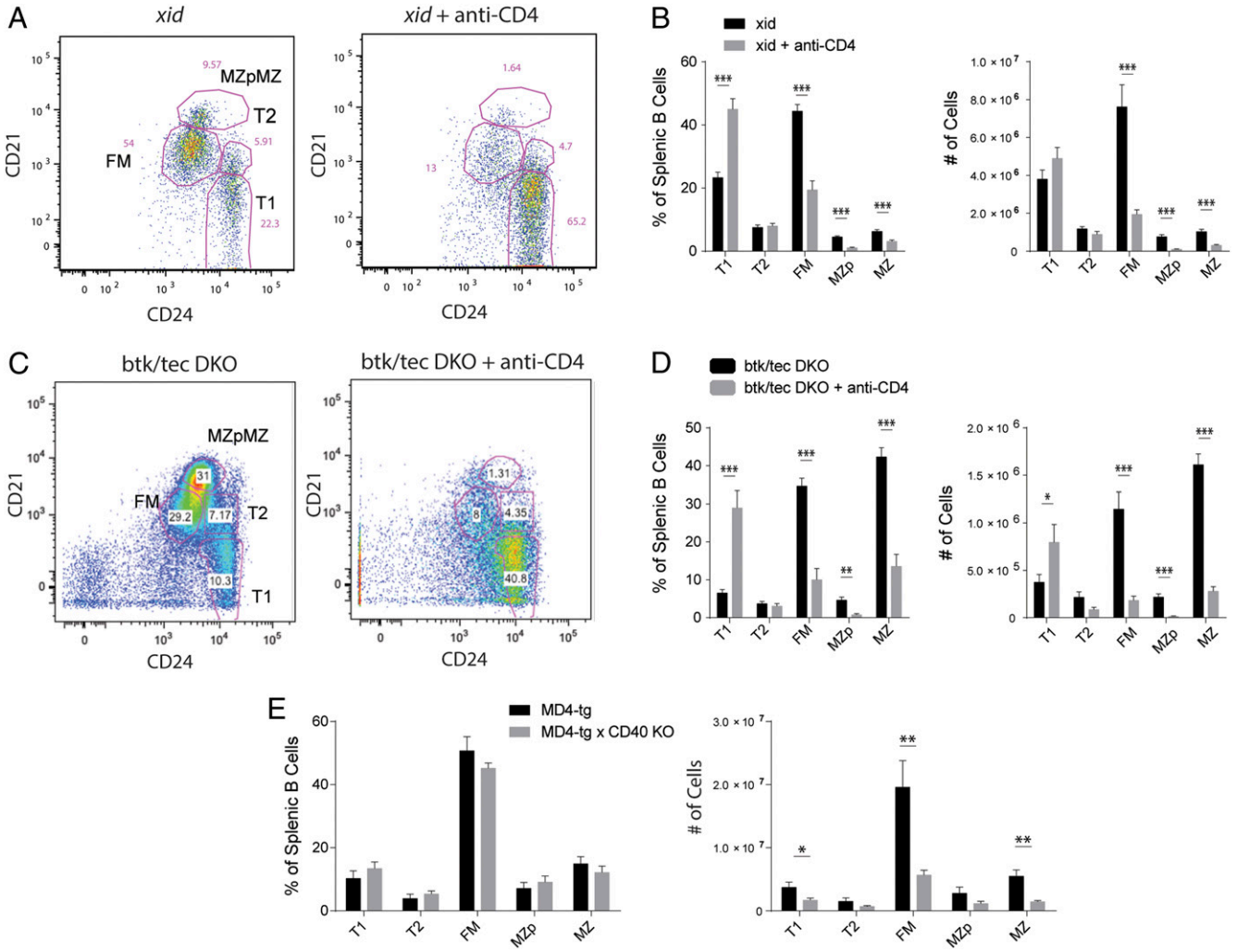

FIGURE 3. B cell development depends on CD40 in the absence of BCR signaling. (**A**) B cell subset gating on *xid* mice (*left panel*) and *xid* mice depleted of CD4 T cells (*right panel*). (**B**) Average splenic B cell subset percentages (*left panel*) and absolute numbers (*right panel*) in *xid* mice and *xid* mice depleted of CD4 T cells. (**C**) B cell subset gating on tec/Btk DKO mice treated with isotype (*left panel*) or CD4-depleting Ab (*right panel*). (**D**) Average splenic B cell subset percentages (*left panel*) and numbers (*right panel*) in tec/Btk DKO mice treated with isotype or CD4-depleting Ab. (**E**) B cell subset percentages (*left panel*) and numbers (*right panel*) in MD4-Tg mice and MD4 × CD40 KO mice. Error bars show SEM. Data representative of at least two experiments. $*p < 0.05$, $**p < 0.005$, $***p < 0.0005$.

PC-specific Id^+ B cells in the MZ pool in the absence of CD40 (12). In M167-Tg mice lacking CD40, the percentage and absolute number of FM cells were reduced, and the percentage of MZ cells was increased (Fig. 4A, 4B). Furthermore, PC-specific MZ B cells were significantly increased in CD40 KO × M167-Tg mice (Fig. 4C, 4D). To account for the possible influence of altered BAFF levels, we created chimeras using BM from M167-Tg mice with and without CD40. Consistent with previous chimera data, CD40 expression provided a competitive advantage to developing B cells, with considerably greater selection pressure than that observed in non–M167-Tg chimeras (Fig. 4E). In these chimeras, both T2 and MZ CD40-deficient subsets contained significantly more Id^+ cells compared with CD40-expressing subsets (Fig. 4F). This supports the idea that in the absence of CD40, population of the naive B cell compartment increasingly depends on Ag-mediated positive selection of transitional cells.

We also assessed selection in M167-Tg WT versus CD40-deficient chimeras based on proliferation history using the KREC assay in MZ cells sorted by both CD40 expression and Id positivity. Although we did not detect differences based on CD40 expression alone, $CD40^{-/-}Id^+$ cells had significantly higher KREC values than $CD40^{-/-}Id^-$ cells (Supplemental Fig. 1D). Consistent with earlier data, CD40-expressing transitional cells had high levels of surface BAFFR and TACI expression (Supplemental Fig. 1E, 1F). However, Id^+ transitional cells had a divergent phenotype with lower BAFFR and higher TACI levels compared with Id^- cells (Supplemental Fig. 1E, 1F). These data demonstrate a key role for CD40 signals in promoting BAFFR expression in transitional cells and suggest an independent role for Ag-mediated BCR signals in this process.

Altered specificity profile of mature B cells in $CD40^{-/-}$ mice

On the basis of the findings from Tg models, we expanded our analysis to the setting of an unrestricted BCR repertoire. Using established methods (43), BCRs were cloned from single FM and MZ B cells sorted from WT and $CD40^{-/-}$ mice. Of 840 sorted

from untreated and CD4-depleted 65:35 CD40 KO:WT mixed BM chimeras; $n = 8$ mice. Error bars show SEM. Data representative of at least three experiments. $*p < 0.05$, $**p < 0.005$, $***p < 0.0005$.

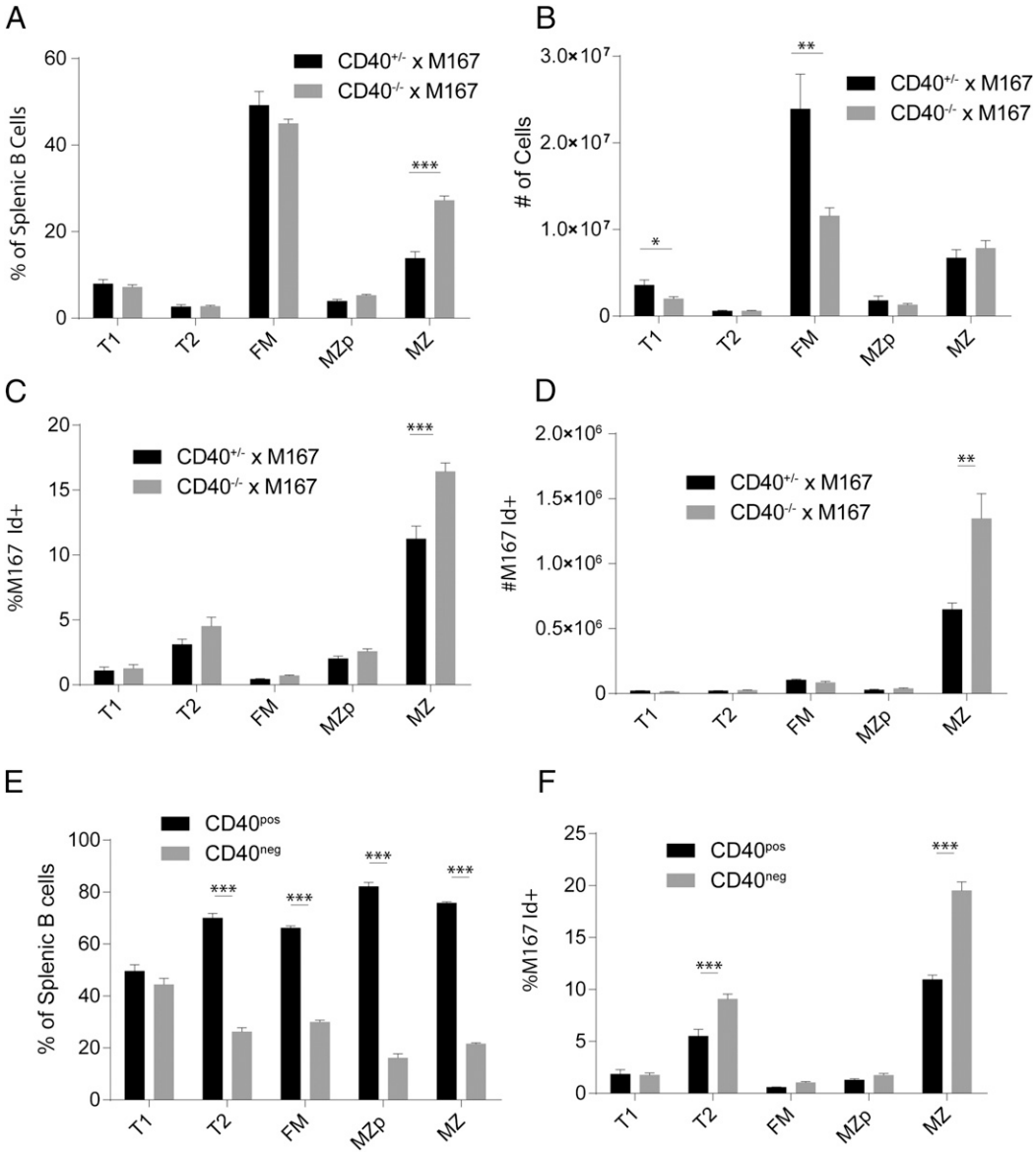

FIGURE 4. Increased Ag-mediated positive selection in the absence of CD40. (**A**–**D**) Selection of Id^+ cells analyzed in $CD40^{-/-}$ × M167-Tg mice versus $CD40^{+/-}$ littermate controls. Comparison of splenic B cell subset percentages (A) and numbers (B). Relative frequency (C) and total number (D) of Id^+ cells in splenic B cell subsets. (**E** and **F**) Analysis of mixed BM chimeras using both $CD40^{+/-}$ × M167 and $CD40^{-/-}$ × M167 donor BM at a ratio of 65:35, respectively. (E) Frequency of $CD40^{pos}$ and $CD40^{neg}$ cells in B cell subsets. (F) Percentage M167 Id^+ cells in $CD40^{pos}$ and $CD40^{neg}$ B cell subsets. Error bars show SEM. Data representative of at least two experiments. $*p < 0.05$, $**p < 0.005$, $***p < 0.0005$.

B cells, 303 rAbs were produced. Following purification, Ab specificity was first evaluated by ANA IFAs, to assess nuclear versus cytoplasmic staining patterns (Supplemental Fig. 3A). Positive ANA staining was detected in 19% of WT versus 21% of $CD40^{-/-}$ FM; and 25% of WT versus 17% of $CD40^{-/-}$MZ Abs (Fig. 5A). Nuclear staining patterns were more frequent in WT MZ (12.5%) versus FM (5.41%)-derived Abs (Fig. 5A). Notably, $CD40^{-/-}$-derived Abs from both subsets displayed reduced nuclear staining (8.43 and 2.35% for MZ and FM, respectively) with proportionally greater cytoplasmic reactivity indicating a subtle alteration in BCR specificity.

Next, we assessed a broad range of potential self-reactive specificities by analyzing pools of cloned Abs using an autoantigen microarray (composed of 88 endogenous Ags associated with Ab-mediated autoimmune diseases). A comparison of normalized, average signals revealed a similar pattern for WT and $CD40^{-/-}$ FM Abs (Fig. 5B). In contrast, the WT MZ Abs exhibited a distinct pattern and reduced overall signal compared with FM Abs, with far fewer Ags generating a detectable signal. $CD40^{-/-}$ MZ Abs exhibited a profile that appeared intermediate between the WT MZ and FM pattern and one that also contained additional unique specificities.

BCR sequences for each recombinant Ab were also assessed according to ANA reactivity using IMGT/VQuest for sequence alignment and the Ig Analysis Tool (IgAT) (39) for generation of descriptive statistics. Notable findings included the following: significantly increased V-D junction N-nucleotide addition (N1 addition) in $CD40^{-/-}$ MZ ANA-positive relative to WT Abs (Fig. 5C); and a tendency, although not significant, for $CD40^{-/-}$ ANA-positive Abs to have shorter CDRH3s (Supplemental Fig. 3C). Thus, individual sequence differences were identified in ANA-positive $CD40^{-/-}$-derived Abs in addition to alterations in staining IFA pattern and specificity profiles.

To determine whether CD40 deficiency impacts enrichment for BCR polyreactivity, Ab specificity was evaluated based on ELISA

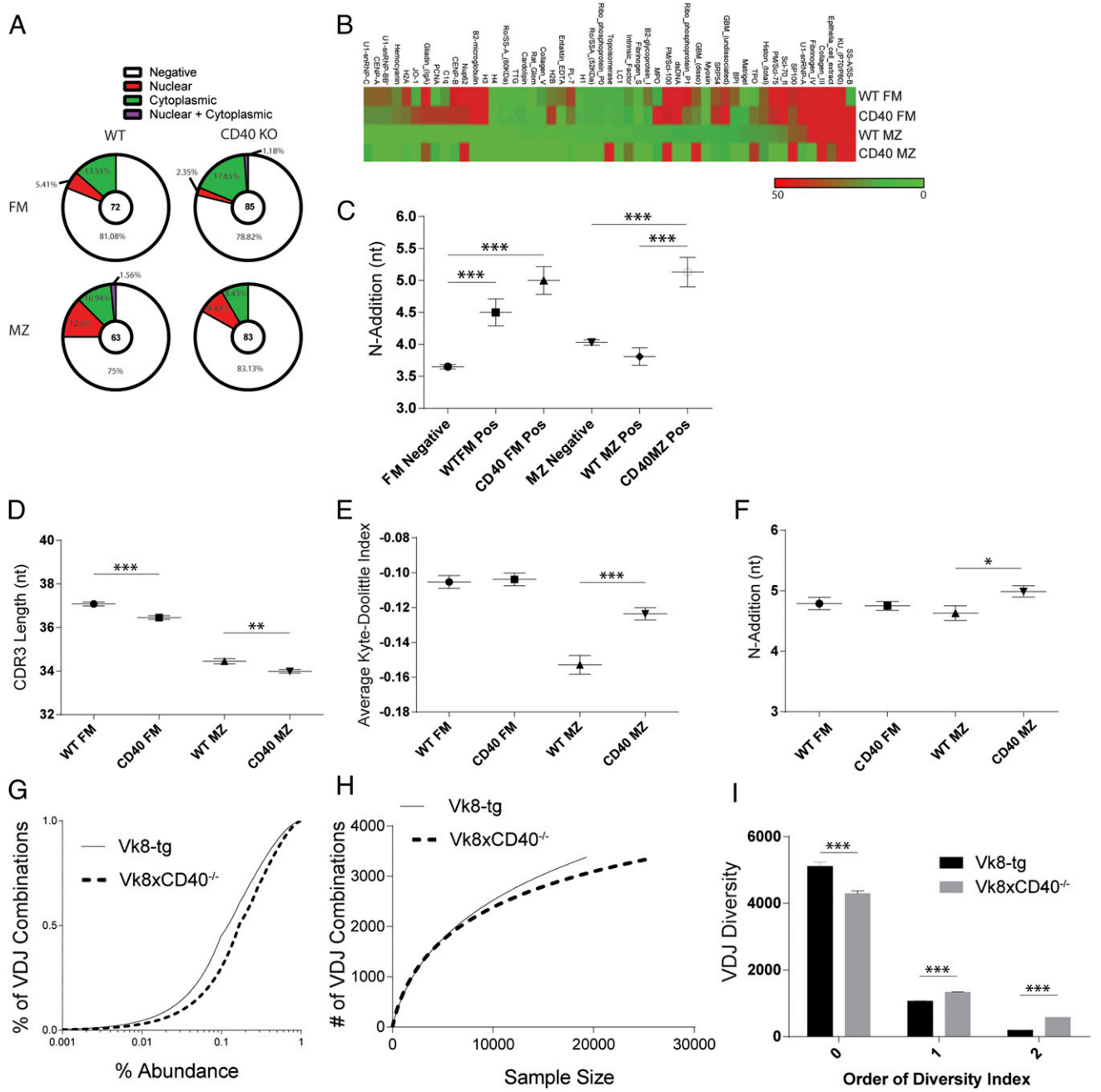

FIGURE 5. Molecular characteristics and specificity profiles of the naive BCR repertoire in WT and CD40 KO mice. (**A**) Relative frequency of each ANA-IFA pattern in cloned BCRs, with total number of Abs evaluated for each subset shown in center of pie charts. (**B**) Autoantigen array data generated using Abs derived from WT versus CD40 KO FM and MZ cells. 60 Abs at equal concentration were pooled for each subset and normalized signal intensities plotted for each Ag. (**C**) BCR IgH sequence characteristics, specifically N-1 addition of cloned rAbs. Total number of BCR clones sequenced are 54 FM negative, 18 WT FM positive, 23 CD40 KO FM positive, 41 MZ negative, 22 WT MZ positive, and 22 CD40 KO MZ positive. (**D**–**F**) High-throughput BCR H chain sequencing of FM and MZ subsets sorted from WT and CD40 KO mice and 90:10 CD40 KO:WT mixed bone marrow chimeric mice. Analysis includes CDRH3 length of WT and CD40 KO mice (D), average Kyte–Doolittle hydrophobicity index (E), and N-1 addition of sorted subsets in mixed BM chimeras (F). (**G**–**I**) BCR diversity analyzed by sequencing splenic B cells derived from Vk8-Tg versusVk8-CD40$^{-/-}$-Tg mice showing empirical cumulative distribution function for VDJ combination frequencies in Vk8-Tg and Vk8CD40$^{-/-}$ B cells (G), individual rarefaction demonstrating the approach to saturation of VDJ combinatorial diversity as sequencing depth increases (H), and diversity index calculations using SPADE (I). Error bars show SEM. Data representative of at least two experiments. *$p < 0.05$, **$p < 0.005$, ***$p < 0.0005$.

assays for ANAs and for three structurally distinct Ags (dsDNA, insulin, and LPS; Supplemental Fig. 2A–C). Abs were classified as polyreactive if positive by ANA ELISA and reactive with at least two additional Ags. 25% of WT FM, 27% of CD40$^{-/-}$ FM, 35% of WT MZ, and 27% of CD40$^{-/-}$ MZ Abs scored as ANA positive by ELISA (Supplemental Fig. 2A–C) (32, 44). Similar to previous data in human naive B cells (43), 4% of WT FM Abs were polyreactive (Supplemental Fig. 3B). In contrast, only 1% of CD40$^{-/-}$ FM Abs were polyreactive. Interestingly, WT MZ–derived Abs exhibited reduced polyreactivity relative to the FM compartment, and CD40$^{-/-}$ MZ–derived Abs completely lacked polyreactivity.

Taken together, these data demonstrate a divergent (and not previously assessed) specificity profile for FM versus MZ B cells in

WT mice and, most notably, alterations in the polarization of such BCR specificities in the absence of CD40.

High-throughput sequencing of BCR H chain genes in WT and CD40$^{-/-}$ mice

To extend the scope of our repertoire analysis, high-throughput sequencing of BCR H chain genes was carried out by pyrosequencing 5′-RACE–generated amplicons. This method was selected to reduce bias induced by using multiple 5′ V-region primers. FM and MZ subsets were sorted from WT and CD40$^{-/-}$ mice as well as WT/CD40$^{-/-}$ mixed BM chimeras, resulting in 3-5 x10^4 sequences per subset, and analysis was restricted to unique clonotypes to avoid PCR amplification-induced bias (Supplemental Table I). Although CD40 deficiency did not alter overall VDJ gene usage (Supplemental Fig. 3D), CD40$^{-/-}$ subsets displayed small but statistically significant decreases in CDRH3 length (Fig. 5D). Although there was no difference in the number of positive or negative CDRH3 charges (data not shown), comparison of average Kyte-Doolittle hydrophobicity (KD) indices revealed a significant increase in the CD40$^{-/-}$ MZ subset compared with WT MZ (Fig. 5E).

An identical analysis was carried out in subsets sorted from WT/CD40$^{-/-}$ mixed BM chimeras. N1 addition was significantly higher in CD40$^{-/-}$ MZ relative to WT MZ sequences (Fig. 5F). Interestingly, in contrast to the non-chimeric setting, the average KD index for the MZ subsets was not significantly different (data not shown); suggesting that mixed BM chimeras may not fully recapitulate normal MZ specificity–based selection. In addition, CD40 deficiency did not affect overall VDJ gene usage (Supplemental Fig. 3D).

Next, we assessed BCR sequence diversity using CD40$^{-/-}$ mice crossed to Vk8-Tg (45) mice to obtain a model wherein H chain variability predominantly determines BCR diversity. Tools developed in ecology to analyze species abundance distributions were applied to sequence data organized, based on VDJ combinations. An empirical cumulative distribution function depicts VDJ abundance in Vk8-Tg and Vk8 × CD40$^{-/-}$ B cells (Fig. 5G). Rarefaction analysis demonstrates that the Vk8 × CD40$^{-/-}$ sample appears to approach a lower theoretical asymptote reflecting fewer total VDJ combinations (Fig. 5H). Finally, the SPADE program was used to calculate zero, first-, and second-order true diversity indices for each population (40, 46). Zero-order diversity was calculated using the Chao-1 estimator (46) and can be interpreted as the predicted total number of VDJ combinations in the sampled subsets. Despite no significant differences in overall VDJ gene selection (data not shown), CD40-deficienct Vk8-Tg mice were estimated to have ~1000 fewer VDJ combinations (5513 for Vk8-Tg versus 4293 for Vk8 × CD40$^{-/-}$; Fig. 5I). These data are consistent with the idea that CD40 supports the survival and selection of particular B cells that, based on their BCR, would otherwise not enter mature compartments.

Discussion

Peripheral selection of developing B cells is critical for the formation of a mature B cell repertoire capable of protecting from infection while minimizing autoreactivity risk. BCR- and BAFF-mediated signals consist of critical regulators of peripheral B cell survival. Our data demonstrate an additional role for CD40, through interaction with CD40L-expressing naive CD4$^+$ T cells, in the survival, developmental progression, and repertoire selection of transitional B cells.

Because transitional B cells are particularly sensitive to lymphopenia-induced HP, a functional HP assay was used to identify novel contributors to peripheral B cell selection. Engagement of CD40 by CD40L on CD4$^+$ T cells consist of a major component of lymphopenia-induced B cell HP. Absence of this signaling axis results in decreased proliferation and stunted phenotypic changes associated with HP reflecting impaired proliferation of either all transferred B cells or a specific subset. This contradicts previous work that concluded HP is T cell independent based on higher HP upon transfer of WT B cells into SCID versus *xid*-recipient mice (47). However, although *xid* mice have partial lymphopenia sufficient to drive B cell HP, total B cell numbers in this strain are substantially greater than in SCID mice and likely explain the authors' findings. Thus, although not absolutely essential for HP, T cells impact the proliferative response to B cell lymphopenia and may be required for HP of specific subsets. We also tested whether Btk influences HP through BCR or TLR signaling as both have been proposed previously (47). Lack of effect on HP using MyD88$^{-/-}$ and TRIF$^{-/-}$ donor B cells demonstrates that Btk operates downstream of BCR signaling in this context, and increased proliferation of PC-specific cells during HP suggests this can be Ag dependent. These data suggest that either T cell help or Ag-induced BCR signaling is sufficient to drive B cell HP. Our observations have important potential clinical implications. Absence of T cell provision of CD40L may result in a decreased rate and altered outcome of B cell reconstitution following hemopoietic stem cell transplant. Consistent with this idea, our unpublished data measuring B cell reconstitution rates in response to sublethal irradiation demonstrates fewer B cells at multiple time points when CD4$^+$ T cells are depleted (as reported by M. Schwartz and D. Rawlings). A recent study also determined that B cell maturation in a humanized mouse model was less efficient in the absence of T cells (33).

Based on these findings, we considered whether CD40 independently supports normal peripheral B cell development. Consistent with prior studies, CD40$^{-/-}$ mice exhibited no alterations in numerical composition of peripheral B cell compartments. Serum BAFF levels were elevated in both CD40$^{-/-}$ and CD40L$^{-/-}$ mice, similar to the increase in serum BAFF in humans lacking CD40L (32), suggesting increased BAFF compensates for the lack of CD40. WT/CD40-mixed BM chimeras were used to directly compare the competitive fitness of WT versus CD40-deficient B cells. We observed a robust competitive advantage for CD40-expressing B cells beginning at the late transitional stage and, most notably, within the MZ subset. Although our study focused on events in the periphery, prior work demonstrated a role for CD40 in BM B cell development (48), which may explain the increased proportion of CD40$^{-/-}$ donor BM required to establish chimeras with equal proportions of early transitional cells. Depletion of CD4$^+$ T cells in these chimeras markedly reduced the competitive advantage of WT transitional B cells. The residual selective advantage for CD40$^+$ cells within the MZ subset after CD4 depletion likely reflects residual CD4$^+$ T cells and/or CD40L expression by non-CD4$^+$ T cells, possibly including myeloid cells.

To investigate how CD40 cooperates with other signals required for transitional development, expression of BAFF family receptors was evaluated in chimeric mice. A striking increase in BAFFR and TACI expression was observed in transitional B cells expressing CD40 versus CD40$^{-/-}$ cells. Correspondingly, expression of pro-survival genes was significantly reduced in CD40$^{-/-}$ versus CD40-sufficient transitional cells. Notably, this phenotype was observed only in the mixed chimera setting. This likely reflects a relative increase in access of WT B cells to limited CD40L, which promotes competitive selection in the presence of CD40$^{-/-}$ transitional cells. Consistent with this idea, the BAFFR phenotype increased in magnitude as the fraction of CD40$^{-/-}$ donor BM increased (data not shown). In summary, CD40 signals promote the transitional B cell developmental program by inducing increased BAFFR expression, leading to enhanced survival signaling.

We next explored the idea that BCR and CD40 signals function independently, yet coordinately, to support peripheral B cell development. First, we tested whether reduced BCR signaling impacts the relative dependence on CD40. Peripheral B cell development is severely reduced in CD4-depleted or CD40$^{-/-}$ *xid* mice, demonstrating increased dependence on CD40 and T cells when BCR signaling is impaired. Using distinct BCR-Tg models, we assessed the role of self-Ag engagement in this process. CD40 deficiency exhibited opposing impact on the fate of HEL-specific B cells (that lack self-reactivity) versus Id^{+} B cells in M167-Tg mice (with affinity for the self-Ag PC). Loss of CD40 signals led to depletion of HEL-specific B cells, whereas PC-specific B cells were specifically enriched. Decreased total FM B cells also were found in CD40$^{-/-}$ × M167-Tg mice, implying that the combined setting of reduced BCR diversity and CD40 deficiency reduces FM B cell selection. These combined findings suggest that 1) a subset of self-Ag–specific B cells are enriched in the absence of CD40, and 2) because BCR diversity is limited, CD40 plays an increasingly important role in B cell development.

To test this model in a physiologic setting with unrestricted B cell diversity, we used single-cell BCR cloning and specificity testing. Our combined findings provide the first direct comparative analysis of the specificity of naive FM and MZ B cell subsets in WT animals. The increased proportion of IFA-reactive and ANA ELISA-positive WT MZ versus FM BCRs is consistent with previous work, suggesting MZ cells are enriched for self-Ag specificity (10, 49, 50). Collectively, our data demonstrate that MZ B cells are enriched for self-reactivity but that such cells use a more restricted spectrum of specificities, implying that a limited set of autoreactive BCRs favors MZ B cell development. In contrast, B cells that express a broader range of specificities, including BCRs with modest polyreactivity, enter the FM subset. Importantly, loss of CD40–CD40L interaction significantly altered these events leading to 1) an alteration in the pattern of IFA reactivity and a decrease in polyreactive FM BCRs, 2) a decreased frequency of autoreactive MZ B cells, and 3) an altered specificity profile of autoreactive B cells in both FM and MZ subsets. Taken together, these findings indicate that deficiency in CD40 signaling impacts the specificity of the naive mature B cell repertoire.

Our findings are partially consistent with results obtained from CD40L-deficient humans but contain several notable differences (32). The modest increase in ANA-positive ELISAs in CD40$^{-/-}$ FMs resembles the increase in ANA reactivity described in mature naive B cells from CD40L-deficient humans, albeit lower in magnitude. However, in contrast to human data, we found reduced polyreactivity and nuclear IFA staining in CD40$^{-/-}$-derived Abs. These differences likely reflect the vastly different environmental exposure encountered by humans compared with mice in specific pathogen-free conditions. In addition, differences in the murine and human repertoire may be because of other B cell survival signals, such as pattern recognition receptor signaling, which may compensate for CD40 deficiency as Myd88-dependent TLR signaling has previously been shown to drive BAFFR expression via TACI (51). Furthermore, we did not extend our analysis past a young age in mice, and it is likely that the effect of CD40 deficiency becomes greater with increasing age. Analyses using additional candidate Ags will be required to gain a more complete understanding of how selection is altered in the CD40-deficient setting.

To expand our analysis of the BCR repertoire to a much larger number of candidate BCRs, we performed high-throughput sequencing of IgH genes. Consistent with altered BCR specificity–based selection in a CD40-deficient setting, we identified key differences in CDRH3 length and KD index values in CD40-deficient BCR sequences consistent with altered BCR specificity–based selection. In addition, IgH combinatorial diversity in Vk8-Tg mice was estimated to decrease by 1000 VDJ combinations in the absence of CD40, indicating a restriction of H chain diversity. Of note, the Vk8-L chain selects for less DNA-reactive BCR clones (52); thus, our Vk8-Tg sequencing data likely underestimate the effect of CD40 deficiency on selection of autoreactive specificities. Collectively, our BCR specificity and high-throughput sequencing data are consistent with a model wherein B cells with particular BCR specificities require CD40 to complete development in the periphery; and that altered specificity-based selection of transitional B cells entering the mature compartment in the absence of CD40 results in reduced BCR diversity.

Taken together, our data support the idea that T cells and CD40 play a key role in peripheral B cell development. On the basis of our findings in lymphopenia models, we predict that B cell reconstitution is likely to be delayed in the absence of sufficient naive CD4^{+} T cells providing CD40L signals. Most notably, although B cell development can proceed in the absence of CD40, this setting does not recapitulate normal selection. Thus, an important implication of our findings is that CD40-mediated shaping of the mature BCR repertoire may facilitate efficient humoral immune responses to neoantigens. Consistent with this idea, many patients have poor responses to pneumococcal vaccines following BM transplant, despite having reconstituted normal B cell numbers, and T cell targeting to mitigate graft-versus-host disease further exaggerates this defect (53). In addition, the altered BCR repertoire generated in the absence of CD40 signals may promote autoimmunity because hyper-IgM patients lacking CD40L suffer from various autoimmune symptoms (54). These collective impacts of the CD40 pathway should be taken into account when considering treatments that suppress T cells or CD40 signals because these manipulations are likely to have previously unappreciated effects on the B cell repertoire. Conversely, modulation of CD40 signaling may also represent a strategy to regulate B cell diversity that might prove useful in the setting of inefficient vaccines, which may elicit stronger responses if the naive BCR repertoire can be temporarily expanded or skewed to enrich for desired germline specificities.

Acknowledgments

We thank Ashok Bandaranayake, Ramit Mehr, David Nemazee, and Tobias Rogosch for help with BCR sequencing and Martin Weigert for providing Vk8-Tg mice. We also wish to acknowledge Patrick Wilson and Sarah Andrews for their help with establishing BCR cloning methodologies.

Disclosures

The authors have no financial conflicts of interest.

References

1. Murphy, K., P. Travers, and M. Walport. 2008. *Janeway's Immunobiology.* Garland Science and Taylor & Francis Group, LLC, New York.
2. Allman, D., and S. Pillai. 2008. Peripheral B cell subsets. *Curr. Opin. Immunol.* 20: 149–157.
3. Loder, F., B. Mutschler, R. J. Ray, C. J. Paige, P. Sideras, R. Torres, M. C. Lamers, and R. Carsetti. 1999. B cell development in the spleen takes place in discrete steps and is determined by the quality of B cell receptor-derived signals. *J. Exp. Med.* 190: 75–89.
4. Allman, D. M., S. E. Ferguson, V. M. Lentz, and M. P. Cancro. 1993. Peripheral B cell maturation. II. Heat-stable antigen^{hi} splenic B cells are an immature developmental intermediate in the production of long-lived marrow-derived B cells. *J. Immunol.* 151: 4431–4444.
5. Rolink, A. G., J. Andersson, and F. Melchers. 1998. Characterization of immature B cells by a novel monoclonal antibody, by turnover and by mitogen reactivity. *Eur. J. Immunol.* 28: 3738–3748.
6. Sater, R. A., P. C. Sandel, and J. G. Monroe. 1998. B cell receptor-induced apoptosis in primary transitional murine B cells: signaling requirements and modulation by T cell help. *Int. Immunol.* 10: 1673–1682.
7. Stadanlick, J. E., and M. P. Cancro. 2008. BAFF and the plasticity of peripheral B cell tolerance. *Curr. Opin. Immunol.* 20: 158–161.

8. Cyster, J. G., J. I. Healy, K. Kishihara, T. W. Mak, M. L. Thomas, and C. C. Goodnow. 1996. Regulation of B-lymphocyte negative and positive selection by tyrosine phosphatase CD45. *Nature* 381: 325–328.
9. Gu, H., D. Tarlinton, W. Müller, K. Rajewsky, and I. Förster. 1991. Most peripheral B cells in mice are ligand selected. *J. Exp. Med.* 173: 1357–1371.
10. Julien, S., P. Soulas, J.-C. Garaud, T. Martin, and J.-L. Pasquali. 2002. B cell positive selection by soluble self-antigen. *J. Immunol.* 169: 4198–4204.
11. Kenny, J. J., A. M. Stall, D. G. Sieckmann, M. C. Lamers, F. D. Finkelman, L. Finch, and D. L. Longo. 1991. Receptor-mediated elimination of phosphocholine-specific B cells in x-linked immune-deficient mice. *J. Immunol.* 146: 2568–2577.
12. Meyer-Bahlburg, A., S. F. Andrews, K. O. A. Yu, S. A. Porcelli, and D. J. Rawlings. 2008. Characterization of a late transitional B cell population highly sensitive to BAFF-mediated homeostatic proliferation. *J. Exp. Med.* 205: 155–168.
13. Zikherman, J., R. Parameswaran, and A. Weiss. 2012. Endogenous antigen tunes the responsiveness of naive B cells but not T cells. *Nature* 489: 160–164.
14. Hayakawa, K., M. Asano, S. A. Shinton, M. Gui, D. Allman, C. L. Stewart, J. Silver, and R. R. Hardy. 1999. Positive selection of natural autoreactive B cells. *Science* 285: 113–116.
15. Wang, H., and S. H. Clarke. 2003. Evidence for a ligand-mediated positive selection signal in differentiation to a mature B cell. *J. Immunol.* 171: 6381–6388.
16. Mackay, F., and P. Schneider. 2009. Cracking the BAFF code. *Nat. Rev. Immunol.* 9: 491–502.
17. Schiemann, B., J. L. Gommerman, K. Vora, T. G. Cachero, S. Shulga-Morskaya, M. Dobles, E. Frew, and M. L. Scott. 2001. An essential role for BAFF in the normal development of B cells through a BCMA-independent pathway. *Science* 293: 2111–2114.
18. Mackay, F., W. A. Figgett, D. Saulep, M. Lepage, and M. L. Hibbs. 2010. B-cell stage and context-dependent requirements for survival signals from BAFF and the B-cell receptor. *Immunol. Rev.* 237: 205–225.
19. Srinivasan, L., Y. Sasaki, D. P. Calado, B. Zhang, J. H. Paik, R. A. DePinho, J. L. Kutok, J. F. Kearney, K. L. Otipoby, and K. Rajewsky. 2009. PI3 kinase signals BCR-dependent mature B cell survival. *Cell* 139: 573–586.
20. Stadanlick, J. E., M. Kaileh, F. G. Karnell, J. L. Scholz, J. P. Miller, W. J. Quinn, III, R. J. Brezski, L. S. Treml, K. A. Jordan, J. G. Monroe, et al. 2008. Tonic B cell antigen receptor signals supply an NF-κB substrate for prosurvival BLyS signaling. *Nat. Immunol.* 9: 1379–1387.
21. Smith, S. H., and M. P. Cancro. 2003. Cutting edge: B cell receptor signals regulate BLyS receptor levels in mature B cells and their immediate progenitors. *J. Immunol.* 170: 5820–5823.
22. Schweighoffer, E., L. Vanes, J. Nys, D. Cantrell, S. McCleary, N. Smithers, and V. L. J. Tybulewicz. 2013. The BAFF receptor transduces survival signals by co-opting the B cell receptor signaling pathway. *Immunity* 38: 475–488.
23. Lesley, R., L. M. Kelly, Y. Xu, and J. G. Cyster. 2006. Naive CD4 T cells constitutively express CD40L and augment autoreactive B cell survival. *Proc. Natl. Acad. Sci. USA* 103: 10717–10722.
24. Khan, W. N., A. Nilsson, E. Mizoguchi, E. Castigli, J. Forsell, A. K. Bhan, R. Geha, P. Sideras, and F. W. Alt. 1997. Impaired B cell maturation in mice lacking Bruton's tyrosine kinase (Btk) and CD40. *Int. Immunol.* 9: 395–405.
25. Oka, Y., A. G. Rolink, J. Andersson, M. Kamanaka, J. Uchida, T. Yasui, T. Kishimoto, H. Kikutani, and F. Melchers. 1996. Profound reduction of mature B cell numbers, reactivities and serum Ig levels in mice which simultaneously carry the XID and CD40 deficiency genes. *Int. Immunol.* 8: 1675–1685.
26. Freitas, A. A., M. P. Lembezat, and B. Rocha. 1989. Selection of antibody repertories: transfer of mature T lymphocytes modifies VH gene family usage in the actual and available B cell repertories of athymic mice. *Int. Immunol.* 1: 398–408.
27. Milićević, N. M., K. Nohroudi, Z. Milićević, H.-J. Hedrich, and J. Westermann. 2005. T cells are required for the peripheral phase of B-cell maturation. *Immunology* 116: 308–317.
28. Wortis, H. H., L. Burkly, D. Hughes, S. Roschelle, and G. Waneck. 1982. Lack of mature B cells in nude mice with X-linked immune deficiency. *J. Exp. Med.* 155: 903–913.
29. Chung, H. Y., Z. Dong, and H. H. Wortis. 1992. B cell deficiency progresses with lineage maturation in nude.X-linked immunodeficient mice B cell deficiency progresses with lineage maturation. *J. Immunol.* 149: 3456–3462.
30. Dong, Z., and H. H. Wortis. 1994. Function of bone marrow stromal cell lines derived from nude mice. *J. Immunol.* 153: 1441–1448.
31. Choudhury, A., P. L. Cohen, and R. A. Eisenberg. 2010. B cells require "nurturing" by CD4 T cells during development in order to respond in chronic graft-versus-host model of systemic lupus erythematosus. *Clin. Immunol.* 136: 105–115.
32. Hervé, M., I. Isnardi, Y. S. Ng, J. B. Bussel, H. D. Ochs, C. Cunningham-Rundles, and E. Meffre. 2007. CD40 ligand and MHC class II expression are essential for human peripheral B cell tolerance. *J. Exp. Med.* 204: 1583–1593.
33. Lang, J., M. Kelly, B. M. Freed, M. D. McCarter, R. M. Kedl, R. M. Torres, and R. Pelanda. 2013. Studies of lymphocyte reconstitution in a humanized mouse model reveal a requirement of T cells for human B cell maturation. *J. Immunol.* 190: 2090–2101.
34. Becker-Herman, S., A. Meyer-Bahlburg, M. A. Schwartz, S. W. Jackson, K. L. Hudkins, C. Liu, B. D. Sather, S. Khim, D. Liggitt, W. Song, et al. 2011. WASp-deficient B cells play a critical, cell-intrinsic role in triggering autoimmunity. *J. Exp. Med.* 208: 2033–2042.
35. van Zelm, M. C., T. Szczepanski, M. van der Burg, and J. J. M. van Dongen. 2007. Replication history of B lymphocytes reveals homeostatic proliferation and extensive antigen-induced B cell expansion. *J. Exp. Med.* 204: 645–655.
36. Andrews, S. F., and D. J. Rawlings. 2009. Transitional B cells exhibit a B cell receptor-specific nuclear defect in gene transcription. *J. Immunol.* 182: 2868–2878.
37. Andrews, S. F., Q. Zhang, S. Lim, L. Li, J.-H. Lee, N.-Y. Zheng, M. Huang, W. M. Taylor, A. D. Farris, D. Ni, et al. 2013. Global analysis of B cell selection using an immunoglobulin light chain-mediated model of autoreactivity. *J. Exp. Med.* 210: 125–142.
38. Tiller, T., C. E. Busse, and H. Wardemann. 2009. Cloning and expression of murine Ig genes from single B cells. *J. Immunol. Methods* 350: 183–193.
39. Rogosch, T., S. Kerzel, K. H. Hoi, Z. Zhang, R. F. Maier, G. C. Ippolito, and M. Zemlin. 2012. Immunoglobulin analysis tool: a novel tool for the analysis of human and mouse heavy and light chain transcripts. *Front. Immunol.* 3: 176.
40. Chao, A., and T. J. Shen. 2010. User's Guide for Program SPADE (Species Prediction and Diversity Estimation). Available at: http://chao stat nthu edu tw/softwareCE html. Accessed May 2013.
41. Kenny, J. J., C. O'Connell, D. G. Sieckmann, R. T. Fischer, and D. L. Longo. 1991. Selection of antigen-specific, idiotype-positive B cells in transgenic mice expressing a rearranged M167-μ heavy chain gene. *J. Exp. Med.* 174: 1189–1201.
42. Rowland, S. L., K. F. Leahy, R. Halverson, R. M. Torres, and R. Pelanda. 2010. BAFF receptor signaling aids the differentiation of immature B cells into transitional B cells following tonic BCR signaling. *J. Immunol.* 185: 4570–4581.
43. Wardemann, H., S. Yurasov, A. Schaefer, J. W. Young, E. Meffre, and M. C. Nussenzweig. 2003. Predominant autoantibody production by early human B cell precursors. *Science* 301: 1374–1377.
44. Tiller, T., J. Kofer, C. Kreschel, C. E. Busse, S. Riebel, S. Wickert, F. Oden, M. M. M. Mertes, M. Ehlers, and H. Wardemann. 2010. Development of self-reactive germinal center B cells and plasma cells in autoimmune FcγRIIB-deficient mice. *J. Exp. Med.* 207: 2767–2778.
45. Prak, E. L., and M. Weigert. 1995. Light chain replacement: a new model for antibody gene rearrangement. *J. Exp. Med.* 182: 541–548.
46. Chao, A. 1984. JSTOR. *Scand. J. Stat.* 11: 265–270.
47. Cabatingan, M. S., M. R. Schmidt, R. Sen, and R. T. Woodland. 2002. Naive B lymphocytes undergo homeostatic proliferation in response to B cell deficit. *J. Immunol.* 169: 6795–6805.
48. Seijkens, T., D. Engel, M. Tjwa, and E. Lutgens. 2010. The role of CD154 in haematopoietic development. *Thromb. Haemost.* 104: 693–701.
49. Li, Y., H. Li, and M. Weigert. 2002. Autoreactive B cells in the marginal zone that express dual receptors. *J. Exp. Med.* 195: 181–188.
50. Wang, H., and S. H. Clarke. 2004. Regulation of B-cell development by antibody specificity. *Curr. Opin. Immunol.* 16: 246–250.
51. Groom, J. R., C. A. Fletcher, S. N. Walters, S. T. Grey, S. V. Watt, M. J. Sweet, M. J. Smyth, C. R. Mackay, and F. Mackay. 2007. BAFF and MyD88 signals promote a lupuslike disease independent of T cells. *J. Exp. Med.* 204: 1959–1971.
52. Ibrahim, S. M., M. Weigert, C. Basu, J. Erikson, and M. Z. Radic. 1995. Light chain contribution to specificity in anti-DNA antibodies. *J. Immunol.* 155: 3223–3233.
53. Bemark, M., J. Holmqvist, J. Abrahamsson, and K. Mellgren. 2012. Translational Mini-Review Series on B cell subsets in disease: reconstitution after haematopoietic stem cell transplantation—revelation of B cell developmental pathways and lineage phenotypes. *Clin. Exp. Immunol.* 167: 15–25.
54. Jesus, A. A., A. J. S. Duarte, and J. B. Oliveira. 2008. Autoimmunity in hyper-IgM syndrome. *J. Clin. Immunol.* 28(Suppl. 1): S62–S66.